Pergamon

PII: S0277-5387(96)00303-8

*Polyhedron* Vol. 16, No. 3, pp. 369–375, 1997

0277–5387/97 $17.00+0.00

# Palladium complexes with simultaneous O : S coordination, syntheses, structures and characterization of complexes with 2-mercaptophenol or 2-mercaptopyridine N-oxide

Ji-Cheng Shi,[a]* Ting-Bin Wen,[a] Yu Zheng,[a] Shi-Jun Zhong,[a] Da-Xu Wu,[a]
Qiu-Tian Liu,[a] Bei-Sheng Kang,[b]* Bo-Mu Wu[c] and Thomas C. W. Mak[c]

[a]State Key Laboratory of Structural Chemistry and Fujian Institute of Research on the Structure of Matter, Chinese Academy of Sciences, Fuzhou, Fujian 350002, P.R. China

[b]Department of Chemistry, Zhongshan University, Guangzhou, Guandong 510275, P.R. China

[c]Department of Chemistry, The Chinese University of Hong Kong, Shatin, New Territories, Hong Kong

(Received 7 May 1996; accepted 22 June 1996)

**Abstract**—Complexes $(Et_4N)_2[Pd_2(mp)_2(Hmp)_2]$ (**1**) and $[Pd(mpo)_2]$ (**2**) synthesized from the reactions of palladium chloride with 2-mercaptophenol ($H_2mp$) and 2-mercaptopyridine N-oxide (Hmpo) or 2,2′-dithiobis(pyridine N-oxide) (dtpo), respectively, have been characterized by X-ray diffraction analyses and studied by IR, Raman, $^1H$ and $^{13}C$ NMR, and EI-MS techniques. The palladium atoms in the two compounds are in square planar environments. The average Pd—O distances are 2.009 Å and 2.043 Å for **1** and **2**, respectively. The results of EHMO calculations show that the Pd—O bonds are weaker than the Pd—S bonds in both compounds and large delocalized $\pi$ bonds extend in the $(mp)_2Pd_2S_2$ plane in **1** and in the $Pd(mpo)_2$ plane in **2**. The reaction of $[Ni(mpo)_2]$ with $[Pd(COD)Cl_2]$ led to the formation of **2** also, which implies that the bidentate O : S ligand mpo readily transfers from the $Ni^{II}$ to the $Pd^{II}$ ion. Copyright © 1996 Elsevier Science Ltd

*Keywords*: palladium complexes; 2R; Raman; NMR; EI-MS; X-ray crystal structures.

Interest in the coordination chemistry of thiolato transition-metal complexes arises in part from the fact that the thiolato group mimics the ligation of cysteinyl residues in proteins [1]. We have studied a series of transition metal complexes with 1,2-bidentate sulfur-containing ligands such as 2-mercaptophenol ($H_2mp$) [2–7] and 2-mercaptopyridine N-oxide (Hmpo) [8–10], of which $H_2mp$ has been found to be a multifunctional ligand in its ligation to transition metal atoms with versatile coordination modes. Recently Zhu *et al.* [11–14] have found that some simple metal complexes, particularly those of palladium complexes containing sulfur ligands, possess the ability of selective-hydrolytic cleavage of proteins and peptides. The regioselectivities of these hydrolyses vary with substrate. The mechanisms are complicated and it is not clear whether the palladium(II) may activate the C—N bond, or deliver $H_2O$. Also, since characterized structures with both Pd—S and Pd—O bonds in the same molecule are rare, it is necessary to study complexes with S and O ligations in detail in order to elucidate the reaction mechanism. This contribution reports the syntheses and physicochemical characterizations of $(Et_4N)_2[Pd_2(mp)_2(Hmp)_2]$ [15] (**1**) and $[Pd(mpo)_2]$ (**2**). EHMO calculations have been carried out, indicating large delocalized $\pi$ bonds extending in the $(mp)_2Pd_2S_2$ plane in **1** and in the $Pd(mpo)_2$ plane in **2**.

## EXPERIMENTAL

Air-sensitive manipulations were carried out under dry dinitrogen. Standard Schlenk-tube, vacuum-line and syringe techniques were utilized. Solvents were

---

* Authors to whom correspondence should be addressed.

dried by standard methods and redistilled before use. 2-Mercaptophenol ($H_2mp$), sodium 2-mercaptopyridine N-oxide (Nampo), 2,2′-dithiobis(pyridine N-oxide) (dtpo) and palladium chloride were all commercially available and used without further purification. [Pd(COD)Cl2] [16] (COD = 1,5-cyclooctanediene) and $[Ni(mpo)_2]$ [8] were prepared by literature methods.

### *Physical measurements and instrumentation*

Elemental analyses were performed by the analytical laboratory of this Institute. Infrared spectra were measured on a Nicolet Magna-750 FT-IR or a Bio-Rad FTS-40 spectrometer, in KBr discs. Raman spectra were recorded on a Nicolet 910 FT-Raman spectrometer using Raman 1064 nm laser source at a resolution of 2 $cm^{-1}$ with 200–400 scans. NMR spectra were measured in DMSO-$d_6$ solutions on a varian Unity-500 spectrometer operating at 499.98 MHz for $^1H$, and 124.71 MHz for $^{13}C$; the internal reference was $SiMe_4$ in all cases (ppm). Mass spectra were obtained at 70 eV on a Finnigan Mat 312 GC-MS spectrometer by the direct inlet method.

### *Preparation of* $(Et_4N)_2[Pd_2(mp)_2(Hmp)_2]$ (**1**)

To a solution of $Na_2mp$ (0.80 g, 5.0 mmol) in absolute EtOH (20 $cm^3$) was added a solution of $[PdCl_2]$ (0.34 g, 2.0 mmol) in MeCN (30 $cm^3$) within 10 min at room temperature. After stirring for 30 min until the color no longer changed, the brown solution was filtered and combined with $Et_4NCl$ (0.50 g, 3.0 mmol) in EtOH (10 $cm^3$). Brown precipitates formed immediately and the solution was kept at 5°C for a few hours and then filtered. The crude product was recrystallized from DMF/MeCN (5 : 1, v/v) to give 0.8 g of brown needle crystals (yield 41%). Found: C, 49.1; H, 5.9; N, 2.6; S, 12.5. Calc. for $C_{40}H_{58}N_2O_4Pd_2S_4$: C, 49.4; H, 6.0; N. 2.9; S, 13.2%. $^1H$ NMR: 11.02 (s, *H*O), 8.79 (dd, $^3J_{16,15}$ = 8.0 Hz, $^4J_{16,14}$ = 1.5 Hz, H16), 6.92 (dt, $^3J_{14,13}$ = 6.5 Hz, $^3J_{14,15}$ = 7.7 Hz, $^4J_{14,16}$ = 1.5 Hz, H14), 6.83 (dt, $^3J_{26,25}$ = 7.2 Hz, $^4J_{26,24}$ = 1.0 Hz, H26), 6.60 (dd, $^3J_{13,14}$ = 6.5 Hz, $^4J_{13,15}$ = 1.5 Hz, H13), 6.58 (dt, $^3J_{24,23}$ = 7.7 Hz, $^3J_{24,25}$ = 7.5 Hz, $^4J_{24,26}$ = 1.0 Hz, H24), 6.55 (dd, $^3J_{15,14}$ = 7.7 Hz, $^3J_{15,16}$ = 8.0 Hz, $^4J_{15,13}$ = 1.5 Hz, H15), 6.31 (dd, $^3J_{23,24}$ = 7.7 Hz, $^4J_{23,25}$ = 1.0 Hz, H23), and 6.29 (dt, $^3J_{25,24}$ = 7.5 Hz, $^3J_{25,26}$ = 7.2 Hz, $^4J_{25,23}$ = 1.0 Hz, H25). $^{13}C$ NMR: 167.0 (C22), 158.4 (C12), 137.1 (C16), 134.6 (C21), 127.2 (C26), 126.3 (C11, C14), 121.7 (C24), 119.3 (C15), 117.8 (C13), 115.3 (C23, C25). IR (CsI, $cm^{-1}$): ν(OH) 3452(w), ν(aryl-H) 3047(m), ν(C=C) 1556(s), ν(C—O) 1230(vs), 1171(s), ν(C—S) 1056(m), 1026(m), ν(Pd—O) 379(m), ν(Pd—S) 313(w), 297(m), 295(m).

### *Preparation of* $[Pd(mpo)_2]$ (**2**)

Route (a): To a suspension of dtpo (0.38 g, 1.5 mmol) and NaOMe (0.10 g, 1.85 mmol) in MeOH/MeCN (50 $cm^3$, 1 : 1, v/v) was added $[PdCl_2]$ (0.18 g, 1.0 mmol). After stirring for 20 h at room temperature, the solution developed a brown color and was filtered. The filtrate gave deep brown prismatic crystals of **2** (yield 60%) on standing at 5°C, which were collected by filtration. Found: C, 33.4; H, 2.1; N, 7.7; S, 17.7. Calc. for $C_{10}H_8N_2O_2PdS_2$: C, 33.5; H, 2.2; N, 7.8; S, 17.9%. $^1H$ NMR: 8.41 (dd, $^3J_{1,2}$ = 6.7 Hz, $^4J_{1,3}$ = 1.2 Hz, H1), 7.62 (dd, $^3J_{4,3}$ = 8.4 Hz, $^4J_{4,2}$ = 1.8 Hz, H4), 7.46 (dt, $^3J_{3,2}$ = 7.2 Hz, $^3J_{3,4}$ = 8.4 Hz, $^4J_{3,1}$ = 1.2 Hz, H3), and 7.18 (dt, $^3J_{2,3}$ = 7.2 Hz, $^3J_{2,1}$ = 6.7 Hz, $^4J_{2,4}$ = 1.8 Hz, H2). $^{13}C$ NMR: 156.4 (C5, C10), 138.0 (C1, C6), 130.9 (C3, C8), 127.8 (C2, C7), 119.5 (C4, C9). IR (CsI, $cm^{-1}$): ν(aryl-H) 3094(m), 3067(m), ν(C=C) 1547(vs), ν(N—O) 1246(vs), ν(C—S) 1042(m), ν(Pd—O) 392(m), ν(Pd—S) 338(w), 315(w), 294(w), 248(m).

Route (b): A mixture of $[PdCl_2]$ (0.18 g, 1.0 mmol) and Nampo (0.60 g, 4.0 mmol) in MeOH/MeCN (80 $cm^3$, 1 : 1, v/v) was stirred for 2 h and filtered. The precipitate was recrystallized from DMF to give brown plate crystals of **2** (yield 72%). The IR spectrum and crystal parameters are identical to that obtained by route (a).

Route (c): To a solution of $Ni(mpo)_2$ (0.08 g, 0.26 mmol) in $CH_2Cl_2$ (10 $cm^3$) was added a solution of $[Pd(COD)Cl_2]$ (0.074 g, 0.26 mmol) in $CH_2Cl_2$ (10 $cm^3$). A yellow precipitate formed immediately and the product **2** was recrystallized from DMF (5 $cm^3$) (yield 65%). The IR spectrum and crystal parameters are identical to that obtained by route (a) or (b).

### *Crystallography*

Intensity data for single crystals of $(Et_4N)_2[Pd_2(mp)_2(Hmp)_2]$ **1** and $[Pd(mpo)_2]$ **2** were collected at room temperature with Mo-$K_\alpha$ radiation (graphite monochromator), $\lambda$ = 0.71073 Å. The data sets were corrected for Lorentz and polarization effects and for absorption employing an analytical procedure. Crystal data are compiled in Table 1.

The structures were solved by the Patterson method and refined by a full-matrix least-squares procedure based on *F*. Final refinement details are also given in Table 1. The maximum residual electron density peaks in the final difference maps are 1.03 e $Å^{-3}$ for **1** and 0.57 e $Å^{-3}$ for **2**, located in the vicinity of the Pd atoms.

### *Molecular orbital calculations*

Extended-Hückel molecular orbital (EHMO) calculations with charge iteration (sense* charge dependence) and weighted $H_{ij}$ were carried out by using the

Table 1. Crystallographic data and data collection parameters for $(Et_4N)_2[Pd_2(mp)_2(Hmp)_2]$ **1** and $[Pd(mpo)_2]$ **2**

| | $(Et_4N)_2[Pd_2(mp)_2(Hmp)_2]$ | $[Pd(mpo)_2]$ |
|---|---|---|
| Formula | $C_{40}H_{58}N_2O_4Pd_2S_4$ | $C_{10}H_8N_2O_2PdS_2$ |
| Colour | Brown plate | Brown plate |
| $M$ | 971.95 | 358.7 |
| Crystal system | Monoclinic | Monoclinic |
| Space group | $P2_1/n$ | $P2_1/n$ |
| $a$ (Å) | 9.088(1) | 8.709(1) |
| $b$ (Å) | 17.851(4) | 14.060(2) |
| $c$ (Å) | 12.932(1) | 10.025(1) |
| $\beta$ (°) | 93.21(1) | 96.79(1) |
| $V$ (Å$^3$) | 2094.7(7) | 1218.9(6) |
| $Z$ | 2 | 4 |
| $D_c$ (g cm$^{-3}$) | 1.54 | 1.955 |
| $\mu$ (mm$^{-1}$) | 1.08 | 1.845 |
| Crystal size (mm$^3$) | $0.35 \times 0.26 \times 0.18$ | $0.15 \times 0.20 \times 0.30$ |
| $F(000)$ | 1000 | 704 |
| Diffractometer | Enraf-Nonius CAD4 | Rigaku RAXIS |
| Temperature (K) | 296 | 293 |
| Scan type | $2\theta$ | $^a$ |
| $2\theta$ range (°) | 49.9 | / |
| No. of unique reflections | $3096(I \geqslant 3\sigma(I))$ | 2128 |
| Weighting scheme | $w = 1/\sigma^2(F)$ | $w = [\sigma^2 F_o + 0.0010 F_o^2]^{-1}$ |
| $R, R_w$ | 0.044, 0.055 | 0.045, 0.070 |

$^a$Take oscillation IP photos; 20 frames in total, $\phi = 0$–180°, $\Delta = 9°$, 15 mins per frame.

ICON 8 version. A total of 164 and 81 valence orbitals involving five $d$ orbitals of Pd were employed for **1** and **2**, respectively. The parameters of Pd atom were taken from [17].

## RESULTS AND DISCUSSION

### *Syntheses*

Excess of mp is necessary to obtain the compound $(Et_4N)_2[Pd_2(mp)_2(Hmp)_2]$ **1**. If the molar ratio of mp : $[PdCl_2]$ is decreased from 2.5 : 1 to 2.0 : 1, a highly air-sensitive crystalline product was isolated, which cannot be identified under present conditions. Treatment of $[PdCl_2]$ with Nampo (route (b)) or with the organic disulphide dtpo under strongly basic condition (route (a)) gave the compound $[Pd(mpo)_2]$ **2**. In the attempt to use the S donor in $[Ni(mpo)_2]$ to coordinate further, it is interesting to find that compound **2** was obtained from the reaction of $[Ni(mpo)_2]$ with $[Pd(COD)Cl_2]$ (eq. 1). This reaction suggests that the bidentate-O : S ligand mpo has transferred from $Ni^{II}$ to $Pd^{II}$, in contrast with bidentate-N : S ligand aminoethanethiolate which transferred from $Pd^{II}$ to $Ni^{II}$ [18].

$$Pd(COD)Cl_2 + Ni(mpo)_2 \rightarrow Pd(mpo)_2 + NiCl_2 + COD \qquad (1)$$

### *Molecular vibration spectra*

The IR and Raman (see Fig. 1) spectra of complex **1** showed the vibrations of C—S bonds appearing at 1056 and 1026 cm$^{-1}$ as two peaks while only one peak at 1042 cm$^{-1}$ was present in **2**. The typical absorptions of C—O bonds for **1** appear at 1230 and 1171 cm$^{-1}$. It is interesting to note that the absorption peaks of the N—O bonds of **2** are both very strong at 1246 cm$^{-1}$ for the IR and Raman spectra and the N—O bending vibration is at 416 cm$^{-1}$. The stretching vibrations of Pd—O bonds have been observed at 378 (IR) and 399, 385 and 366 cm$^{-1}$ (Raman) for **1** and

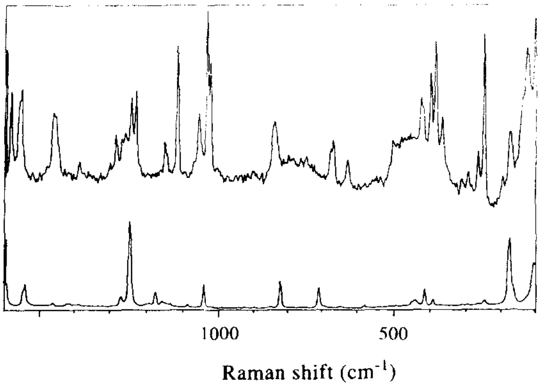

Fig. 1. Raman spectra of compounds **1** (upper) and **2** (lower).

391 $cm^{-1}$ (IR and Raman) for **2**, which are comparable to the values of 395–340 $cm^{-1}$ in triangulo-hexa-$\mu$-acetatopalladium(II) [19] and are lower than that of 464 $cm^{-1}$ in acetylactonatopalladium(II) [20]. The Pd—S stretching vibrations are in the range of 313–295 $cm^{-1}$ for both **1** and **2** in their molecular vibration spectra, consistent with $\nu$(Pd—S) (388–240 $cm^{-1}$) [21,22]. It also seems reasonable to assign bands in the range of 100–140 $cm^{-1}$ to O—Pd—S bending vibrations.

### *EI-MS characterization*

The molecular ion peak of **1** in a positive EI-MS spectrum was not observed, but the fragment $[Pd(Hmp)_2]^+$ peak with low abundance (2%) appeared and decomposed to produce the ions $[Pd(Hmp)_2$—$O]^+$ (45%), $[Pd(Hmp)_2$—$CO]^+$ (3%) and $[Pd(Hmp)_2$—$Cs]^+$ (4%). Ions $[PdO(S)]^+$ (100%) and $[PdS]^+$ (29%) were also observed together with one of the major ions $[Hmp]^+$ (56%). The MS spectrum of $[Pd(mpo)_2]$ **2** is similar to the other complexes containing mpo ligand [23] with the ions: $M^+$ (100%), [$M^+$—O] (5%), [$M^+$—2O or S] (9%), [$M^+$—SC] (85), [$M^+$—2S] (2%), [$M^+$—2O—2S] (6%), [$M^+$—mpo] (3%), [$M^+$—mpo—O] (20%), [$M^+$—mpo—S] (8%), [$M^+$—mpo—CS] (88%), [$M^+$—mpo—S—O] (25%), $[PdO(S)]^+$ (5%), $[mpo]^+$ (4%) and $[mpo—O]^+$ (6%).

### *NMR spectra*

The $^1H$ and $^{13}C$ NMR spectra of complex **2** are easy to assign, however, those of the dinuclear anion of **1** cannot be analyzed simply owing to the fact that the mp ligands is of the ABCD system and in the two kinds of terminal and bridging coordination modes. The $^1H$ signals overlap in the region of 6–7 ppm, and only ten $^{13}C$ signals appear in its $^{13}C$ NMR spectrum although there should be twelve inequivalent carbons, in which the signals at 126.3 and 115.3 ppm may be the overlapped peaks estimated roughly from their intensity. Consequently, some 2D NMR techniques have been applied to assign the NMR spectra.

The signal at 11.03 ppm comes from the hydroxy proton of the bridging mp ligand which forms a strong intermolecular hydrogen bond with the oxygen atoms of the terminal mp ligand [O(1)···O(2*), 2.596 Å]. This fact indicates clearly that the dinuclear anion also exists in the DMF solution. The other $^1H$ signals in the region of 6–9 ppm can be assigned into two groups: 8.79 [H(16)], 6.92 [H(14)], 6.60 [H(13)], and 6.55 [H(15)]; 6.83 [H(26)], 6.58 [H(24)], 6.31 [H(23)], and 6.29 [H(25)], by the $^1H$–$^1H$ COSY and simulated spectra. However, which group of signals are contributed by the bridging or terminal mp ligand cannot be assigned. Then the $^1H$–$^{13}C$ HMBC (Heteronuclear Multiple Bond Connectivity) spectrum was recorded [24]. The $^1H$ signal at 11.03 ppm of hydroxy proton correlates to the $^{13}C$ one at 117.8 ppm [C(13)] in $^1H$–$^{13}C$ HMBC spectrum, and the C(13) signal also correlates to the signal at 6.60 [H(13)] ppm in the $^1H$–$^{13}C$ HMQC spectrum (Fig. 2), suggesting that the former group signals should be ascribed to the protons of the bridging mp ligand and the latter group to the terminal mp ligand.

The $^{13}C$ signal at 115.3 ppm correlates to both H(23) and H(25) in the HMQC spectrum, implying that the 115.3 ppm signal is contributed from both C(23) and C(25). Accordingly, the C(13) (117.8), C(14) (126.3), C(15) (119.3), C(16) (137.1), C(24) (121.7), and C(26) (127.2) were assigned. In the HMBC spectrum, the $^{13}C$ signal at 126.3 ppm [contributed partially from C(14)], not only correlates to H(16) owing to the result of C(14), but also to H(13) and H(15), demonstrating that the 126.3 ppm signal is also contributed from C(11). The last three signals: 167.0 ppm correlating to H(26) and H(24), 158.5 to H(16) and H(14), and 134.6 ppm to H(25) and H(23) in the HMBC spectrum, indicate that they are C(22), C(12), and C(21), respectively.

### *Description of the structures*

The molecular structures of the anion $[Pd_2(mp)_2(Hmp)_2]^{2-}$ of **1** and the compound $[Pd(mpo)_2]$ **2** are illustrated in Figs 3 and 4, respectively. Selected structural parameters are listed in Tables 2 and 3.

The dinuclear anion of **1** consists of two equivalent molecular fragments related by a crystallographic inversion center. The two Pd, four S, two O atoms and the two phenyl rings in the terminal ligands are essentially coplanar, while the planes of the two phenyl rings in the bridging ligands are tilted by 68.6° from the $mp_2Pd_2S_2$ plane. The structure is quite similar to that reported for $(Et_4N)_2[Ni_2(mp)_2(Hmp)_2]$ [2].

The molecule of **2**, which is also quite similar to that of $[Ni(mpo)_2]$ [8], has a palladium atom in the centre of the nearly square planar $PdS_2O_2$ unit with the two mpo ligands in the *cis* configuration. The whole molecule exhibits a *pseudo*-$C_{2v}$ symmetry with

Table 2. Selected atomic diatances (Å) and bond angles (°) for the anion $[Pd_2(mp)_2(Hmp)_2]^{2-}$ of **1**

| | | | |
|---|---|---|---|
| Pd—O(2) | 2.009(3) | Pd—S(2) | 2.280(1) |
| Pd—S(1) | 2.295(1) | Pd—S(1*) | 2.349(1) |
| S(1)—C(11) | 1.796(5) | S(2)—C(21) | 1.773(5) |
| O(1)—C(12) | 1.353(7) | O(2)—C(22) | 1.358(6) |
| O(2)—Pd—S(2) | 86.6(1) | O(2)—Pd—S(1) | 176.7(1) |
| O(2)—Pd—S(1*) | 91.4(1) | S(2)—Pd—S(1) | 96.30(5) |
| S(2)—Pd—S(1*) | 177.99(6) | S(1)—Pd—S(1*) | 85.72(5) |
| C(11)—S(1)—Pd | 107.9(2) | C(11)—S(1)—Pd(*) | 105.4(2) |
| Pd—S(1)—Pd(*) | 94.28(5) | C(21)—S(2)—Pd | 96.8(2) |
| C(22)—O(2)—Pd | 118.0 | | |

Symmetry operator: *, $1-x$, $-y$, $1-z$.

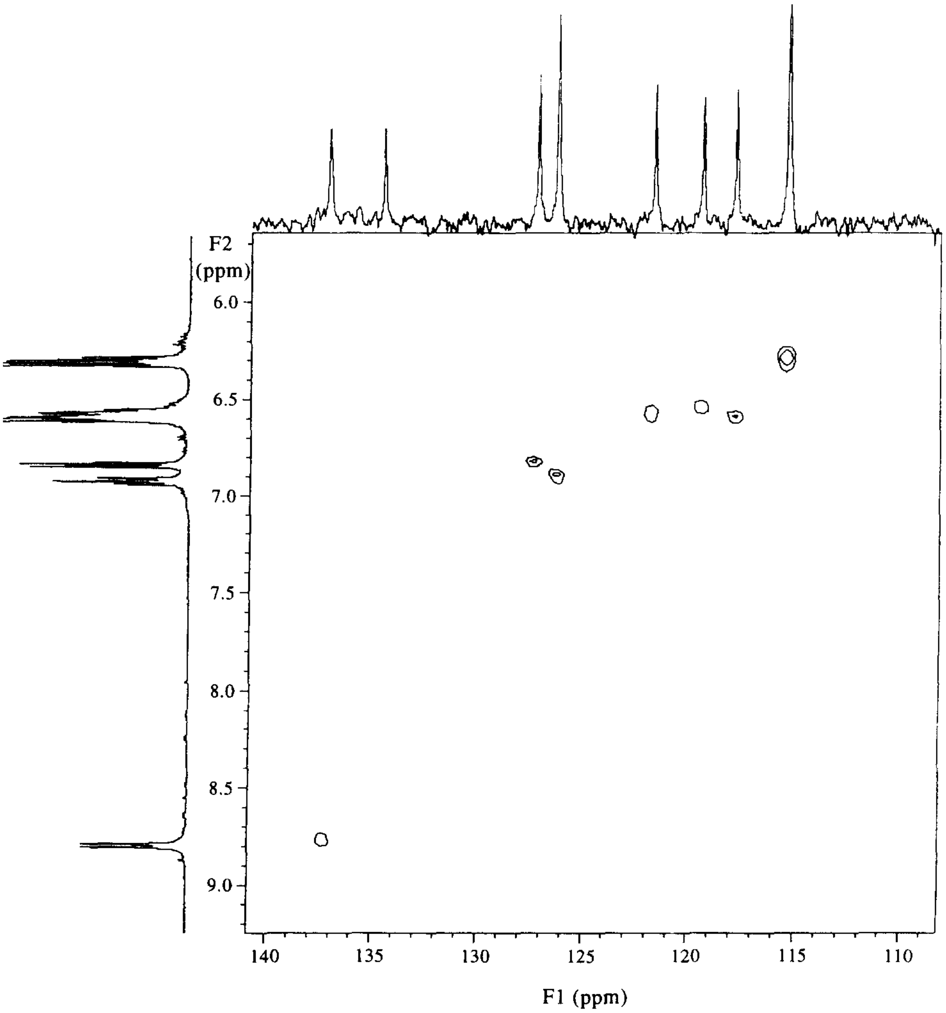

Fig. 2. $^1H$–$^{13}C$ HMQC spectrum of **1**.

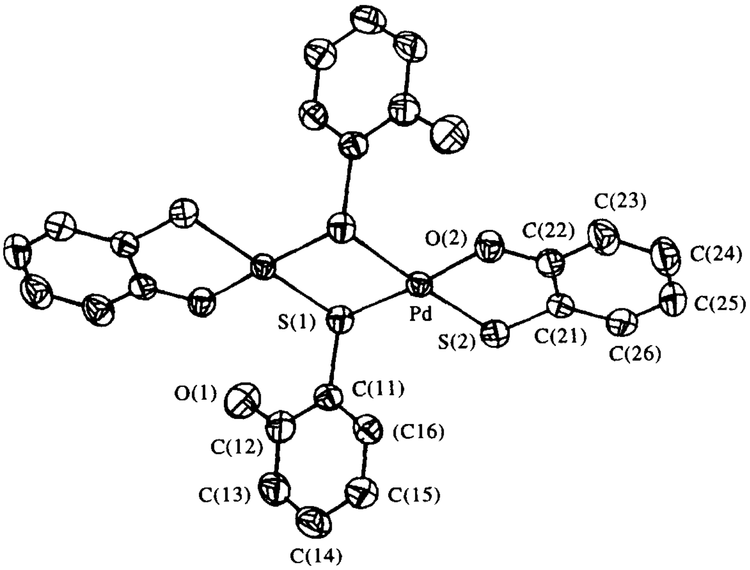

Fig. 3. Structure of anion $[Pd_2(mp)_2(Hmp)_2]^{2-}$ **1** with atom numbering scheme.

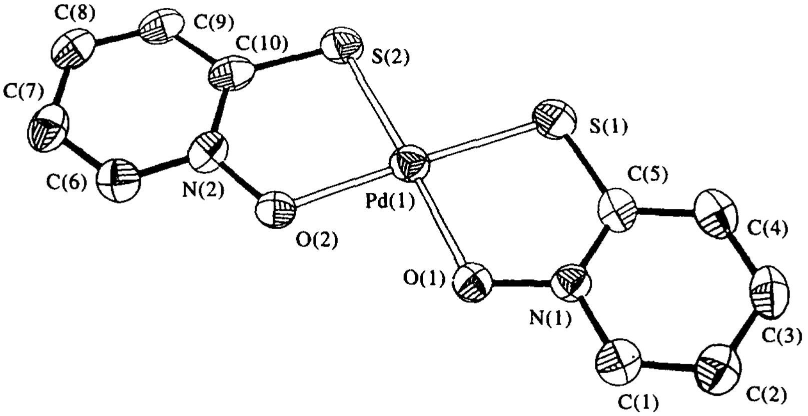

Fig. 4. Structure of [Pd(mpo)$_2$] **2** with atom numbering scheme.

the $C_2$ axis passing through the palladium atom and the mid-points of S(1)···S(2) and O(1)···O(2).

The Pd—S bond length of av. 2.412 Å of **2** are somewhat longer than those terminal (2.280 Å) and bridging (av. 2.322 Å) Pd—S bonds of **1**, and than that reported (2.296 Å) [25]. The Pd—O bond of av. 2.043 Å in **2** is also slightly longer than that in **1** (2.009 Å) and that in the tetrachlorocatechol complex $[Pd(C_6Cl_4O_2)(PPh_3)_2]$ (av. 2.033 Å) [26], and than the values reported for [Pd{PhC(O)CC(O)Me}$_2$] (1.98 Å) [27]. The long Pd···Pd* distance of 3.404(1) Å indicates that a Pd···Pd* bonding interaction seems unlikely. The relatively short C—S distances (av. 1.73 Å) in **2** show partial double bond character as they are nearly 0.1 Å shorter than the normal covalent distance (1.81 Å) [28] for a C—S single bond, and also definitely shorter by 0.04–0.05 Å than that in **1**. This feature results in the fact that complexes with mpo ligands have little ability to bridge another metal ion through the sulfur atom to form polynuclear complexes. The bite angles O—Pd—S of **2** (85.6°) are smaller than that in **1** (86.6°). The Pd—S—C angle of 96.8° for **1** of the terminal ligand, and of 98.0° (average) for **2** show the bonding orbital of the chelating sulfur atoms are mainly of *p* character, and the oxygen atom of Pd—O—C (118.0°) in **1** and of Pd—O—N (115.8°) in **2** show more of $sp^2$ character.

Table 3. Selected atomic distances (Å) and bond angles (°) for [Pd(mpo)$_2$], **2**

| | | | |
|---|---|---|---|
| Pd—S(1) | 2.241(2) | Pd—O(1) | 2.042(4) |
| Pd—S(2) | 2.243(2) | Pd—O(2) | 2.045(5) |
| S(1)—C(5) | 1.741(6) | O(1)—N(1) | 1.351(7) |
| S(2)—C(10) | 1.720(7) | O(2)—N(2) | 1.356(7) |
| N(1)—C(1) | 1.353(8) | N(1)—C(5) | 1.339(7) |
| S(1)—Pd—O(1) | 85.6(1) | S(1)—Pd—S(2) | 95.8(1) |
| O(1)—Pd—S(2) | 178.4(1) | S(1)—Pd—O(2) | 178.0(1) |
| O(1)—Pd—O(2) | 92.5(2) | S(2)—Pd—O(2) | 86.1(1) |
| Pd—S(1)—C(5) | 97.9(2) | Pd—O(1)—N(1) | 115.8(3) |
| Pd—S(2)—C(10) | 98.2(2) | Pd—O(2)—N(2) | 115.8(3) |

## *Theoretical calculations*

The Pd—O bonds with the average bond order 0.275 and 0.277 for **1** and **2**, respectively, are a lot weaker than the Pd—S bonds (av. 0.458 and 0.408 for **1** and **2**, respectively).

The HOMO at −10.806 eV of the anion of **1** consisting of the atomic orbital: Pd(1.4%), O(3.4%), S(17.6%) and C(74.8%), shows that the HOMO involves 23% *d-p* $\pi$ component and 77% C—C $\pi$ component. The LUMO at −9.469 eV contains the atomic orbital: Pd(36.9%), O(23.6%) and S(37.2%), in which *d-p* $\pi^*$ character is obvious.

The HOMO at −11.380 eV of **2** contains: Pd(3.9%), O(33.1%), S(24.4%) and C(34.9%), involving 63.7% *d-p* $\pi$ and 36.3% C—C $\pi$ components. Similar to that of **1**, the LUMO at −9.466 eV consisting of the atomic orbitals: Pd(33.8%), O(16.5%) and S(42.3%), shows also significant *d-p* $\pi^*$ character.

The facts mentioned above indicate that there are some large delocalized $\pi$ bonds extending in the $(mp)_2Pd_2S_2$ plane in **1** and in the Pd(mpo)$_2$ plane in **2**. The energy gap (1.915 eV) between LUMO and HOMO in the anion of **1** is larger than that of **2** (1.337 eV), which suggests that the mixing of the *d-p* $\pi$ with $\pi$ of the phenyl ring is better in **1** than in **2**.

*Acknowledgements*—This work was supported by the Climbing Program-State key Project for Fundamental Research, the National Natural Science Foundation of China and the Hong Kong Research Grants Council Earmarked Grant No. CUHK 311/949.

## REFERENCES

1. B. S. Kang, Q. T. Liu, and J. X. Lu, *Nitrogen Fixation Research in China* (Edited by G. F.

Hong) Ch. 6, p. 151. Springer–Verlag, Heidelberg (1992).

2. B. S. Kang, L. H. Weng, D. X. Wu, F. Wang, Z. Guo and H. Q. Liu, *Inorg. Chem.* 1988, **27,** 1128.
3. B. S. Kang, L. H. Weng, D. X. Wu, L. R. Huang, F. Wang, Z. Guo and H. Q. Liu, *Inorg. Chim. Acta* 1988. **148,** 147.
4. B. S. Kang, L. H. Weng, H. Q. Liu, L. R. Huang, D. X. Wu, C. Z. Lu, J. H. Cai, X. T. Chen and J. X. Lu, *Inorg. Chem.* 1990, **29,** 4873.
5. X. T. Chen, H. Q. Liu, L. H. Weng, L. R. Huang, D. X. Wu, X. J. Lei and B. S. Kang, *J. Coord. Chem.* 1991, **22,** 109.
6. B. S. Kang, X. T. Chen, L. H. Weng, L. R. Huang, C. Z. Lu and J. X. Lu, *Science in China* (*chi.*) *Ser. B* 1991, 18.
7. B. S. Kang, Y. J. Xu, X. L. Xie, C. N. Chen, Q. T. Liu and J. X. Lu, *Inorg. Chem.* 1994, **33,** 3770.
8. X. T. Chen, Y. H. Hu, D. X. Wu, L. H. Weng and B. S. Kang, *Polyhedron* 1991, **10,** 2651.
9. Y. H. Hu, L. H. Weng, L. R. Huang, X. T. Chen, D. X. Wu and B. S. Kang, *Acta Cryst., Sect. C* 1991, **47,** 2655.
10. B. S. Kang, Y. J. Xu, J. H. Peng, D. X. Wu, X. T. Chen, Y. H. Hu, M. C. Hong and J. X. Lu, *Polyhedron* 1993, **12,** 871.
11. L. Zhu and N. M. Kostic, *Inorg. Chem.* 1992, **31,** 3994.
12. L. Zhu and N. M. Kostic, *J. Am. Chem. Soc.* 1993, **115,** 4539.
13. L. Zhu and N. M. Kostic, *J. Am. Chem. Soc.* 1994, **116,** 5218.
14. L. Zhu and N. M. Kostic, *Inorg. Chim. Acta* 1994, **217,** 21.
15. Structural data has already been communicated: J. S. Shi, X. Y. Huang, T. B. Wen, Y. H. Deng, C. N. Chen, Q. T. Liu and B. S. Kang, *Jiegou Huaxue* 1995, **14,** 293.
16. R. Ros, G. Garturan and G. Mauro, *Trans. Met. Chem.* 1976, **1,** 13.
17. J. K. Burdett and T. Hughbarks, *J. Am. Chem. Soc.* 1984, **106,** 3101.
18. T. Konno, K. Yonenobu, J. Hidaka and K. Okamoto, *Inorg. Chem.* 1994, **33,** 861.
19. L. Soptrajanova and B. Soptrajanov, *Spectroscopy Lett.* 1992, **25,** 1131.
20. M. Mikami, I. Nakagawa and T. Shimanouchi, *Spectrochim. Acta* 1968, **24A,** 1291.
21. J. Sola and R. Yaner, *J. Chem. Soc., Dalton Trans.* 1986, 2021.
22. D. M. Roundhill, *Inorg. Chem.* 1980, **19,** 557.
23. Y. H. Hu, X. T. Chen, L. Dai, L. H. Weng and B. S. Kang, *Jiegou Huaxue* 1993, **12,** 38.
24. D. X. Wu, J. C. Shi and B. S. Kang, *Chinese J. Magnetic Resonance* 1996, **13,** 377.
25. J. P. Beale and N. C. Stephenson, *Acta Cryst. Sect. B* 1972, **28,** 557.
26. C. G. Pierpoint and H. H. Downs, *Inorg. Chem.* 1975, **14,** 343.
27. S. Okeya, S. Oei, K. Matsumoto and Y. Nakamura, *Bull. Chem. Soc. Jpn.* 1981, **54,** 1085.
28. J. D. Lydon, R. C. Elder and E. Deutsch, *Inorg. Chem.* 1982, **21,** 3168.